BCI training effects on chronic stroke correlate with functional reorganization in motor-related regions: A concurrent EEG and fMRI study

Kai Yuan
Chinese University of Hong Kong
Cheng Chen
Chinese University of Hong Kong
Xin Wang
Chinese University of Hong Kong
Winnie Chiu-wing Chu
Chinese University of Hong Kong
Kai Yu Tong (kytong@cuhk.edu.hk)
Chinese University of Hong Kong https://orcid.org/0000-0003-4375-653X

Research

Keywords: brain computer interface, stroke, robot hand training, EEG, fMRI, functional connectivity, effective connectivity

Posted Date: April 21st, 2020

DOI: https://doi.org/10.21203/rs.3.rs-22395/v1

RESEARCH

BCI training effects on chronic stroke correlate with functional reorganization in motor-related regions: A concurrent EEG and fMRI study

Kai Yuan[1†], Cheng Chen[1†], Xin Wang[1], Winnie Chiu-wing Chu[2] and Kai-Yu Tong[1*]

Correspondence:
ytong@cuhk.edu.hk
Department of Biomedical Engineering, The Chinese University of Hong Kong, Shatin, Hong Kong
Full list of author information is available at the end of the article
Equal contributor

Abstract

Background: Brain-computer interface (BCI) guided robot-assisted training strategy has been increasingly applied to stroke rehabilitation, while few studies have investigated the neuroplasticity change and functional reorganization after intervention from multi-modality neuroimaging perspective. The present study aims to investigate the hemodynamic and electrophysical changes induced by BCI training using functional magnetic resonance imaging (fMRI) and electroencephalography (EEG) respectively, as well as the relationship between the neurological changes and motor function improvement.

Method: 14 chronic stroke subjects received 20 sessions of BCI-guided robot hand training. Simultaneous EEG and fMRI data were acquired before and immediately after the intervention. Seed-based functional connectivity for resting state fMRI data and effective connectivity analysis for EEG were processed to reveal the neuroplasticity changes and interaction between different brain regions. Moreover, the relationship among motor function improvement, hemodynamic changes and electrophysical changes derived from the two neuroimaging modalities were also investigated.

Results: This work suggested: (a) significant motor function improvement could be obtained after BCI training therapy; (b) training effect significantly correlated with functional connectivity change between ipsilesional M1 (iM1) and contralesional Brodmann area 6 (including *premotor area* (cPMA) and *supplementary motor area* (SMA)) derived from fMRI; (c) training effect significantly correlated with information flow change from cPMA to iM1 and strongly correlated with information flow change from SMA to iM1 derived from EEG; (d) consistency of fMRI and EEG results illustrated by the correlation between functional connectivity change and information flow change.

Conclusions: Our study showed changes in the brain after the BCI training therapy from chronic stroke survivors and provided a better understanding of neural mechanisms, especially the interaction among motor-related brain regions during stroke recovery. Besides, our finding demonstrated the feasibility and consistency of combining multiple neuroimaging modalities to investigate the neuroplasticity change. This study was registered at https://clinicaltrials.gov (NCT02323061) on 23 December 2014.

Keywords: brain computer interface; stroke; robot hand training; EEG; fMRI; functional connectivity; effective connectivity

Introduction

Stroke is the leading cause of death and one of the main causes of acquired adult disability [1]. The most common and widely recognized impairment caused by stroke is motor impairment, which can be regarded as a loss of function in muscle control or movement or a limitation in mobility [2]. A majority of patients have impaired upper-limb (UL) motor function following stroke and have difficulty in independently performing daily-living activities. Therefore, one of the challenging aspects of stroke rehabilitation is UL intervention [3]. Neuroplasticity is a term describing the property of human brain to adapt to environmental pressure, experiences, and challenges including brain damage [4]. It extends to many levels from molecules to cortical reorganization. [5]. Various novel stroke rehabilitative methods for motor recovery, such as robotic therapies and noninvasive brain stimulation, have been developed based on basic science and clinical studies characterizing brain remodeling due to neural plasticity [6, 7]. Task-specific, high-intensity exercises in an active, functional, and highly repetitive manner over a large number of trials have been shown to enhance motor recovery [8, 9]. Robot-assisted therapy is highly repetitive, intensive, adaptive and quantifiable, which focuses on ameliorating the impaired limb in line with concept of neuroplasiticity [10]. A robot-assisted therapy with well-designed tasks was illustrated in one recent study [11], where promising long-term training effect in the motor function was observed in chronic stroke subjects.

Brain-computer interface (BCI) technology has been used for rehabilitation after stroke for years [12]. The majority of these studies are case reports of patients who operated a BCI to control either rehabilitation robots [13–15] or functional electrical stimulation (FES) [16, 17]. EEG electrodes placed over the sensorimotor regions are often selected to control the external device since they provide the most localized and reliable functional cortical activation changes relevant to the hand's motor function. Specifically, the neurophysiological phenomena of event-related desynchronization or synchronization (ERD/ERS) [18] can be detectable from EEG of stroke patients while performing motor imagery (MI) or motor execution (ME) tasks. With real-time processing, triggers will be sent to control an FES generator or exoskeleton robotic device [19]. BCI implies learning to modify the neuronal activity through progressive practice with contingent feedback and reward [20]. Therefore, changes in functional cortical activation patterns could remain when performing

similar tasks as the BCI training even after the completion of the therapy [21]. In spite of some promising results achieved so far, BCI stroke rehabilitation is still a young field where different works report variable clinical outcomes [22]. The necessary functional connectivity changes among brain regions induced in stroke patients with lasting recovery effect remain unclear, with only several putative mechanisms been proposed [23].

It is now well established that many functional networks in human brain are consistent across subjects, including sensory networks (visual, auditory, somatosensory) and sensorimotor network, as well as some associative 'control' networks (default mode, dorsal attention, fronto-parietal, ventral attention) [24–26]. Functional connectivity (FC) which measures the temporal correlation of the blood oxygen level dependent (BOLD) signal between different regions at rest has emerged as a powerful tool to map the functional organization of the brain. Studies imply that different behavioral impairments following stroke are related to the disruptions of communication in distributed brain networks with corresponding particular behavioral domains [27]. Furthermore, there is a growing awareness that disrupted functional interactions, especially inter-hemispheric interactions, are highly correlated with motor behavioral deficits and post-stroke recovery [28–31].

Although correlation-based connectivity using fMRI can investigate the relationship between distant brain regions, this kind of connectivity cannot provide any precise information related to the directionality of the information flow due to its poor time resolution. Electroencephalograph (EEG) is a prominent tool which offers a more direct measure of the electrophysiological signal with higher time resolution to explore the dynamic brain processes [32]. EEG signal can be regarded as the integration of all concurrently active sources in the brain [33]. Effective connectivity developed from Granger-causality theory can be derived from EEG signal. This kind of connectivity reveals the directed information flow from one region to another and embeds both correlation and directional information between brain areas [34]. Among measures estimating effective connectivity, generalized partial directed coherence (GPDC) has shown good performance and is able to diminish the influence of noise [35]. Different from fMRI with poor temporal resolution or fluctuations in hemodynamic response, EEG is more suitable to capture the effective connectivity through this approach. To date, few studies focused on utilizing the effective connec-

tivity change to characterize or predict the rehabilitation training effect for stroke subjects and meanwhile, multiple neuroimaging modalities were seldom combined simultaneously to investigate the brain recovery mechanism induced by training therapy.

In this study, two neuroimaging modalities, including EEG and fMRI, were employed to evaluate the neuroplasticity changes in chronic stroke subjects after interventions using BCI robot hand training paradigm. Motor function of the paretic upper-limb of stroke subjects was evaluated at three time points: before, immediately after and 6 months after the interventions. Seed-based functional connectivity from resting-state fMRI and effective connectivity analysis from EEG were investigated to reveal the changes in neuroplasticity and interaction between different brain regions. Moreover, we also investigated the correlation between connectivity changes in two neuroimaging modalities and motor function changes after interventions. In the end, we explored the relationship between hemodynamic changes revealed by fMRI data and electrophysical changes revealed by EEG data. These findings may provide us with a better understanding of neural mechanisms during stroke recovery from BCI training and with guidance to future experimental design for upper limb. To our best knowledge, this is the first study to utilize concurrent EEG and fMRI to investigate the BCI training effect.

Materials and Methods

Subject

Fourteen chronic stroke patients (13 males, mean age = 54±8 years) with the right (n=9) or left (n=5) hemisphere impaired were recruited from local community. The inclusion criteria were: (1) first-ever stroke, (2) onset of stroke diagnose more than 6 months prior to the beginning of individual experiment trial, (3) a single unilateral brain lesion, (4) sufficient cognition and comprehensive ability to understand and perform corresponding tasks tested by Mini–Mental State Examination (MMSE) with score > 21, (4) moderate to severe motor dysfunctions for the paretic upper extremity (Fugl-Meyer Assessment score for upper-extremity < 47)[36] and (5) no additional rehabilitation therapies applied to the patient. Exclusion criteria were: (1) aphasia, neglect, and apraxia, history of alcohol, drug abuse, or epilepsy, (2)

severe hand spasticity, (3) hand deformity and wound, (4) bilateral infracts, uncontrolled medical problems, and (5) serious cognitive deficits.

Motor functions of the paretic upper limbs for all stroke subjects were assessed with Fugl-Meyer Assessment for upper-extremity (FMA) at three time points: before (Pre), immediately after (Post) and 6 months after (Six-month) the intervention respectively, by the same experienced clinical assessor who was blinded to the subjects' rehabilitation training. Table 1 summarizes the demographics and clinical properties of the stroke subjects. The lesion distribution of stroke patients is shown in Figure 1(C).

BCI Motor Imagery Training System

A BCI motor training system was designed as shown in Figure 1(A). The EEG signals of each subject were acquired by 16 electrodes (g.LADYbird, g.Tec Medical Engineering GmbH, Austria), amplified by an amplifier (g.USBamp, g.Tec Medical Engineering GmbH, Austria), and then processed by a connected computer immediately. A paradigm with fixed sequence showing instructions for motor imagery was played to guide the subject to complete a training task (shown in Figure 1(D)). An exoskeleton robot hand was used to assist the paretic hand to accomplish grasp or open tasks. From fully extended position to fully flexed position, the fingers assembly provided 55 degrees and 65 degrees range of motion (ROM) for the MCP and PIP finger joints respectively. When under no load, the maximum contraction speed of the robotic hand was approximately 2 seconds to fully open or closed positions of the robotic hand. During each trial, the subjects were asked to relax for 2 s followed by a white cross for 2 s to remind the subjects to do preparation. A text cue of 'hand grasp' or 'hand open' was then displayed for 2 s to illustrate the following motion. After that, the subjects were instructed to conduct motor imagery while a video clip with a duration of 6 s was displayed simultaneously for guidance. The trigger to the robot hand was sent based on the α suppression of EEG signal during the motor imagery to assist the subjects to complete grasp/open task in the following 3 s. Afterwards, the α suppression score as the feedback was displayed for 2 s on the screen after robot hand execution to guide the subjects to achieve higher scores in the following trials. Finally, a 2-second rest was given to the subjects. Trials were repeated with grasping and opening tasks appeared alternately. During

the training, sixteen EEG electrodes were placed over the central area according to the international 10–20 system (C1, C2, C3, C4, C5, C6, Cz, FC1, FC2, FC3, FC4, FCz, CP1, CP2, CP3, CP4). EEG signals were referenced to unilateral earlobe, grounded at the location of Fpz, and sampled at 256 Hz. The sampling signals were further processed in real-time using band-pass filter (2–60 Hz) and notch filter (48–52 Hz) to remove artifacts and power line noise, respectively. All electrodes were filled properly with conductive gel to ensure all the impedances were kept below 5 kΩ. Similar with other studies [37, 38], EEG signals from C3 and C4 channels were used for BCI control and meanwhile, all channels were used to generate the real-time topography of the brain dynamic potential for surveillance.

Alpha suppression reflects an event-related desynchronization (ERD) of the EEG caused by an increase in neural activity [39], which has been widely utilized in BCI training field and has promising outcome [40, 41]. The α rhythm is mainly found over the vertex (near location of Cz) or laterally across the precentral motor cortex, normally at C3 or C4 electrode depending on which hand or arm movement is being performed. To compute α suppression, C3 or C4 channel was chosen according to the subject's lesion side. The EEG data were transferred to frequency domain by a fast Fourier transform with a Hanning window, covering the EEG data during the motor imagery period (6s) in paradigm. The mean power in the α band (8–13 Hz) of the selected electrode was calculated. Then the α suppression score was calculated using the following Equation [42]:

$$\alpha_{SS} = -\frac{P_{MI} - P_{rest}}{P_{rest}} \times 100 \tag{1}$$

where α_{SS} stands for the α suppression score, P_{MI} stands for the α power of EEG during motor imagery, and P_{rest} stands for the α power of EEG during resting state. The robot hand was triggered to apply a mechanical force to help hand grasp or open if the α suppression score is more than 20, which means the ratio of α power between motor imagery and rest was below 80% according to the average results of healthy subjects [43].

Interventional Protocols

All subjects received a 20-session BCI robot hand training with an intensity of 3–5 sessions per week. The whole training process was completed within 5–7 weeks. At

the beginning of each training session, the subject was asked to sit in a height-adjustable chair and the trainer would standardize the posture to keep his/her shoulder naturally flexed and abducted, elbow flexed at 90 degree, arm pronated but wrist positioned neutrally without any flexion or extension. The subjects were instructed to try to maintain the standard posture during the whole training. During each session, 100 repetitive hand movements were performed by each subject with intermittent rest after every 10 trials. A robot hand was used to provide mechanical support to assist the subject in completing hand grasp or open task. Subjects were asked to imagine either grasping or releasing a cup following the instruction. Robot hand was triggered to help hand open or grasp if α suppression score calculated from real-time EEG signals was above 20 at α_{SS}. The overall success rate was 85.3% $\pm$ 6.4 %, with the range from 72.9% to 95.8%. All subjects were instructed to imagine the same movement with the affected hand during the stimuli display. The subjects would be reminded to conduct motor imagery if evidence of attempting movements was observed. The EMG activity was also monitored by the trainers. The experimental sequences for the training paradigm was developed based on Psychophysics Toolbox 3.0 (http://psychtoolbox.org/).

MRI and EEG Data Acquisition

MRI scans were acquired for all subjects before and after the intervention. A 3T Philips MR scanner (Achieva TX, Philips Medical System, Best, Netherlands) with an 8-channel head coil was used to acquire high resolution T1-weighted anatomical images (TR/TE = 7.47/3.45 ms, flip angle = 8°, 308 slices, voxel size = 0.6 $\times$ 1.042 $\times$ 1.042 mm^3) using a T1-TFE sequence (ultrafast spoiled gradient echo pulse sequence), and BOLD fMRI images (TR/TE = 2,000/30 ms, flip angle = 70°, 37 slices/volume, voxel size = 2.8 $\times$ 2.8 $\times$ 3.5 mm^3) using a FE-EPI sequence (gradient echo echo-planar-imaging sequence). Both resting-state and task-based fMRI were acquired. The sequences were displayed using EPrime 2.0 (Psychology Software Tools, PA USA). When acquiring resting-state fMRI, subjects were presented with a white crosshair in black background and instructed to rest while focusing on the fixation cross during the fMRI acquisition. The resting state fMRI acquisition lasted for 8 min. When acquiring task-based fMRI, subjects were asked to try to do grasp and open using their paretic hand when a mark of "L" or "R" (decided by each

subject's paretic hand) appeared on the screen and were also asked to maintain 6 seconds until the mark disappeared from the screen. An event-related design was adopted and randomized time intervals from 14 to 20 seconds were assigned between every two tasks. Two 6-minute task-based fMRI runs were performed for each subject.

The EEG data were acquired simultaneously with the fMRI using Neuroscan system (SynAmps2, Neuroscan Inc, Herndon, USA). The MR-compatible EEG cap was placed with 64-channel Ag/AgCl EEG electrodes according to standard 10-20 system, as well as 2 extra electrocardiogram (ECG; left lower and near-midline upper chest) electrodes and 1 electrooculogram (EOG; below right eye) electrode. All recording impedances were kept below 5 kΩ. The reference channel was located at the point between Cz and CPz; AFz electrode was treated as ground. Signals were filtered between 0.1 and 256 Hz using analog filter and sampled at 1000 Hz for off-line processing.

MRI Data Analysis

MRI Data Preprocessing

The resting-state fMRI data were preprocessed using the Data Processing Assistant for Resting-State fMRI (DPARSF) toolbox [44] based on Statistical Parametric Mapping (SPM8) (http://www.fil.ion.ucl.ac.uk/spm). The first 10 volumes were discarded to assure the remaining volumes of fMRI data were at magnetization steady state. The remaining volumes were corrected with slice timing and realigned for head motion correction. Nuisance variables were then regressed out including white matter, cerebrospinal fluid (CSF), global mean signal and Fristion 24 head motion parameters [45]. To further control for head motion, scrubbing process were done for the volumes with framewise displacement (FD) value exceeed 0.3 [46]. Then the anatomical dataset was aligned to the functional dataset. Detrending and temporal band-pass filtering (0.01 Hz - 0.1 Hz) [47, 48] were performed to remove higher frequency physiological noise and lower frequency scanner drift. Subsequently, the functional images were spatially normalized to the Montreal Neurological Institute (MNI) template (MNI152: average T1 brain image constructed from 152 normal subjects), resliced to 2 mm × 2 mm × 2 mm voxels, and smoothed with a Gaussian kernel with a full-width at half-maximum (FWHM) of 6 mm. In order to do group

statistical analysis later, subjects with left-hemispheric lesions were flipped along the midsagittal plane using MRIcron (www.mccauslandcenter.sc.edu/mricro/mricron), which was also adopted in other studies [49, 50], so that the lesions of all subjects were in the right hemisphere.

The task-based fMRI data were also preprocessed using DPARSF toolbox. Similar preprocessing steps were performed on task-based fMRI data except that the threshold for FD value was set to 0.7 in the motion scrubbing step [51] and no band-pass filter was used. Subjects with left-hemispheric lesions were also flipped along the midsagittal plane.

Seed-Based FC Analysis

In order to avoid the bias induced by a prior determination of seeds based on a hypothesis or prior results, seed locations were decided based on task-fMRI. At the intra-subject level, general linear model (GLM) was applied to voxel-level to estimate the statistical parametric maps of the t-statistic for each subject. At the inter-subject level, one-sample t-test was performed on the individual t-maps. The statistical threshold was set at $P < 0.05$ (corrected for multiple comparison). The group activation map is shown in Figure 2(A). We defined two spherical seeds with radius of 5 mm surrounding the highest activation vertex from the task-based results. The ipsilesional M1 (iM1) seed location was set at (38, -22, 56) in MNI space and contralesional M1 (cM1) was set symmetrically at (-38, -22, 56) in MNI space with also referenced to some other studies [52, 53].

In this study, we focused on motor-related areas for seed-based analysis. The average time course of the BOLD signal within the seeds during each resting-state scan was calculated and used as the regressors of interest in a subject-level general linear model (GLM) to assess the FC of each ROI with every other voxel in the brain. The seeds were checked one subject by one subject to ensure that they did not contain any lesioned voxels. This analysis produced maps of all voxels that were positively or negatively correlated with a seeds' mean time courses.

After calculating individual seed-based correlation maps, paired t-test was performed for each seed to see whether there were significant changes in FC brought by training effect. Corrections for multiple comparison at the cluster level were carried out using Gaussian random field theory (minimum $Z > 2.7$; cluster-wise

significance: $P < 0.05$, corrected). To correct for multiple seeds, we only considered the clusters that had a probability greater than $P = 0.05/2$ (2 was the number of seeds) as significant clusters [54]. All the analysis for mixed effect model and paired t-test were carried out in DPARSF toolbox [44]. We also explored whether the changes in functional connectivity in brain were correlated with the assessment score changes. Pearson correlation coefficients were calculated between FMA score changes and the FC changes between seed area (ipsilesional M1) and corresponding areas (contralesional BA6 area) with which the FC has significantly changed (see Figure 3) after 20 sessions of robot hand training.

EEG Analysis

EEG Preprocessing

EEG data were processed mainly with EEGLAB [55], Fieldtrip toolbox [56], Matlab signal processing toolbox and custom-made codes (Mathworks Natick, MA, USA). Under the condition where MRI was acquired simultaneously, the switching of magnetic field gradients would pollute and overwhelm EEG signal which led to low signal to noise ratio (SNR). A principle component analysis (PCA)-based optimal basis set (OBS) algorithm [57] was adopted to remove the MRI gradient artifact and the onset markers indicating the beginning of each fMRI volume, generated by MRI scanner were also provided for better extraction and selection of artifactual features. The output EEG signal were double-checked visually to ensure that the amplitude was not grandiosely large. The time course of heartbeat artifact was determined with a R-peak detection algorithm [58]. The final ECG artifact was eliminated channel-wisely using the strategy which combined independent component analysis, OBS and an information-theoretic rejection criterion developed by Liu and colleagues [58].

After that, EEG signal was band-pass filtered from 2 to 40 Hz using a Butterworth non-causal filter. Subsequently, bad channels were removed and reconstructed using spherical spline interpolation with neighbor electrodes. Following that, all data were common average referenced. According to the fMRI trigger markers, these data were segmented into non-overlapping two-second epochs where the first and last several data segments were removed due to signal instability. Bad epochs were rejected based on statistical measurement metrics(e.g. z-score, variance, min, and

max etc.) with remaining ones further inspected visually to guarantee the signal quality. We utilized adaptive mixture independent component analysis (AMICA) algorithm [59] to separate EEG signals into spatially static and maximally temporally independent components [60]. The components related to residual artifact induced by MRI scanning, Electrooculogram (EOG) artifact and muscular artifact were rejected. Processes of remaining components were then projected back to all original channels.

Finally, we applied a surface Laplace filter with the spherical spline method [61] to increase the topographical selectivity, eliminate the volume conduction and highlight the high-spatial-frequency components while attenuating low ones [62]. For group-level analysis convenience, all EEG for those patients with left-hemisphere lesion was left-right flipped before signal processing procedure.

Effective Connectivity analysis

Based on the fMRI results, three regions of interest (ROIs) were determined for further effective connectivity analysis, i.e. contralesional premotor area (cPMA), supplementary motor area (SMA) and ipsilesional primary motor area (iM1). Several representative EEG electrodes overlying these three ROIs were carefully selected, *FC3* and *C3* for cPMA, *CZ* and *FCZ* for SMA and *C4* for iM1[63].

To extract the directional information transformation between the above ROIs, generalized partial directed coherence (GPDC), a multivariate (MV) approach based on Granger causality [64], was adopted. It was developed to circumvent the numerical problem related to time series scaling and is more robust for less clean signal[65]. Basically, GPDC is derived from the MV autoregressive (MVAR) model [66] using an appropriate order to fit the time series data. MVAR model is described as following:

$$\mathcal{X}(n) = \sum_{k=1}^{p} A(k)\mathcal{X}(n-k) + \mathcal{W}(n) \tag{2}$$

where $\mathcal{X}$ is the time series, p is the model order, k is the time lag, $A(k)$ is the fitting coefficient given time lag k and $\mathcal{W}(n)$ is the residual white and uncorrelated noise. Leveraging the estimated model coefficients with the input noise variance into

consideration, the value of GPDC can be calculated as:

$$GPDC_{ij}(f) = \frac{\frac{1}{\sigma_i^2}|A_{ij}(f)|^2}{\sum_{m=1}^{M}\frac{1}{\sigma_m^2}|A_{mj}(f)|^2} \tag{3}$$

where f is the frequency, $\sigma_i(\sigma_m)$ is the ith (mth) diagonal element of the residual noise covariance matrix, and $A_{ij}(f)$ is the coefficient transformed to the frequency domain which is related to interaction between the ith and jth signal.

GPDC can be treated as a measure of directional information or interaction from one signal to another with explicit directionality, which is different from conventional coherence [67] characterizing the indirect and undirected couplings. Given frequency f, the *Information Flow (IF)* from $ROI_j(\Omega_j)$ to $ROI_i(\Omega_i)$ for EEG can be further determined by incorporating GPDC values:

$$IF_{ij}(f) = IF_{i\leftarrow j}(f) = \frac{\sum_{m\in\Omega_i}\sum_{n\in\Omega_j} GPDC_{mn}(f)}{N_i N_j} \tag{4}$$

where Ω represents the ROI. $GPDC_{mn}$ indicates the GPDC value calculated between EEG signals from electrode m (in ROI_i) and electrode n (in ROI_j) respectively with the direction from electrode n to electrode m. N_i means the number of representative electrodes in ROI_i. Given the direction in a pair of ROIs, ROI_i and ROI_j can be considered as *sink* region and *source* region of information flow respectively.

In our study, we used a MVAR model of order 10 corresponding to 40 ms of the signal to fit the EEG data, which is consistent with previous studies [68, 69]. The value of GPDC and information flow were calculated separately for each epoch and then averaged over all epochs as better performance was found in this way than by extracting a single MVAR model from the aggregated data of all epochs, according to previous studies [70]. In the frequency domain, we mainly focused on 8 to 30 Hz which contained two essential brain oscillatory activity frequency bands, alpha band (8-12 Hz) and beta band (12-30Hz) [71]. Furthermore, all GPDC and information flow values were averaged across all frequency bins.

Similar with fMRI analysis, iM1 was selected as seed ROI but with two possible roles (*sink* region or *source* region). Pearson correlation coefficients were calculated between FMA score changes and the information flow change between cPMA and iM1 as well as between SMA and iM1 before and after training. Besides, the

correlations between FC change (between iM1 and BA6 area) and corresponding information flow change were also investigated to inspect whether similar changes were associated between the findings from these two neuroimaging modalities.

Statistics

Statistic analyses were performed using SPSS 25.0 (IBM SPSS Statistics, NY, US) with the significance level set at $p < 0.05$. Friedman test at time level (Pre, Post and Six-month) was applied to examine whether FMA score was changed after the intervention. Friedman test is a non-parametric test which was widely adopted to assess differences over time in clinical scores including FMA in recent studies [72–74]. Wilcoxon signed ranks test was used as post-hoc test to examine significant changes of different combinations of three time-points for FMA score. Pearson correlation coefficients were used to test the relationship between FMA score changes and the connectivity changes from two neuroimaging modalities. Bonferroni corrections were used for multiple comparisons.

Results

Friedman tests with time (Pre, Post and Six-month) as within-subject factor indicated that significant effect of time was observed for FMA score ($p = 0.005$). Post-hoc Wilcoxon signed ranks tests for FMA score indicated that there were significant increases in FMA scores between Pre and Post ($p = 0.004$) as well as between Pre and Six-month ($p = 0.015$), no significant change was found between Post and Six-month ($p = 0.878$). The result was illustrated in Figure 1(B). The results indicated that BCI robot hand training was able to promote motor recovery with a long-term effect.

For the functional connectivity analysis with seed ROI at iM1, paired t-test showed that significant clusters were observed in contralesional Brodmann area 6 (BA6: *premotor cortex* and *supplementary motor area*). This suggested that the functional connectivity between iM1 and contralesional BA6 was significantly increased after 20 sessions of BCI robot hand training (Figure 2C). Pearson correlation analysis further revealed that the FC changes between iM1 and contralesional BA6 was significantly correlated with the FMA score changes ($r = 0.64$, $p = 0.013$, Figure 3) after BCI robot hand training. There was no significant cluster survived after multiple comparison correction for the paired t-test when the seed ROI was at cM1.

Due to the lack of accurate fMRI triggers, the EEG signals of two subjects were not further analyzed to avoid processing bias, resulting in 12 subjects with both EEG and fMRI scans. Therefore, EEG analysis was only conducted on the remaining 12 subjects. First of all, we investigated the topography of the information flow change when iM1 was treated as either the sink or the source regions. Figure 4 illustrates the two conditions (iM1 as *sink*/*source* region), where both premotor area and supplementary motor area showed notably changed patterns after the intervention. This phenomenon was more obvious and continuous when iM1 acted as the receiver of the information flow.

Then we explored the relationship between training effect and information flow changes when iM1 was treated as a sink region (i.e. information flow from cPMA or SMA to iM1). The results are illustrated in Figure 5. Pearson correlation analysis revealed that information flow change from cPMA to iM1 significantly correlated with the FMA score change after BCI robot hand training ($r = 0.6963$, $p = 0.0476$, Bonferroni corrected). The information flow change from SMA to iM1 correlated strongly with FMA score change ($r = 0.6046$, $p = 0.1492$, Bonferroni corrected, $p = 0.0373$, uncorrected), although not significantly. However, from the opposite direction, neither information flow change from iM1 to cPMA ($r = -0.405$, $p = 0.7660$, Bonferroni corrected) nor from iM1 to SMA ($r = 0.1189$, $p = 1$, Bonferroni corrected) correlated significantly or strongly with FMA score change.

Upon determining the sink region role of iM1 in predicting training effect, we involved the FC changes from fMRI into correlation analysis. As illustrated in Figure 6, there is a significant association between the information flow change from cPMA to iM1 and their FC change ($r = 0.6902$, $p = 0.0260$, Bonferroni corrected) as well as a strong relationship between the information flow change from SMA to iM1 and FC change ($r = 0.5859$, $p = 0.1167$, Bonferroni corrected).

Discussion

This study investigated the neuroplasticity change and functional reorganization after BCI-guided robot-assisted training intervention from multi-modality neuroimaging perspective. Besides, the relationship between the neurological changes and motor function improvement was also investigated. Our study showed the change in the brain after BCI training therapy for chronic stroke survivors and provided a

better understanding of neural mechanisms, especially the interaction among motor-related brain regions during stroke recovery using MRI and EEG. The correlation finding demonstrated the feasibility and consistency of combining multiple neuroimaging modalities to investigate the neuroplasticity change. Furthermore, our findings can provide insights into the design of stroke rehabilitation therapies for clinical application.

Non-invasive BCI systems have been introduced for upper limb rehabilitation after stroke for years, coupling with other interventions like occupational/physical therapy. Some studies reported significant motor function improvement after training with the help of BCI [22, 75]. Biasiucci et al. illustrated that BCI coupled with FES elicited significantly better motor recovery than sham FES in chronic stroke patients. Furthermore, the underlying mechanism might relate to the FC between ipsilesional motor areas from neuroplasticity perspective. Kim et al. used combined action observational training (AOT) plus BCI-based FES (BCI-FES) as the experimental training therapy and found that the combination of AOT plus BCI-FES with conventional therapy is more effective comparing to sole conventional therapy in term of upper limb motor improvement. Our study integrated brain-computer interface and robot hand, which further resembled such findings by exhibiting a significant training effect after 20 sessions of BCI robot hand training in chronic stroke. The feedback offered by BCI facilitates the appraisal of performance by enforcing the sensory aspect in the sensorimotor loop [76]. External devices like robotic hand could provide haptic as well as proprioceptive feedbacks on the intended movement, thereby restoring the 'action–perception coupling'. In this way, BCI robot-assisted training has already been shown to induce neuroplasticity [77]. Using intention with robotics training showed effective motor function improvement. Besides, the cortical area corresponding to hand is larger than the area corresponding to elbow or shoulder [78]. Distal joint training might involve larger brain areas to induce neuroplasticity modulation. However, it is noted that, from our study we did not claim the training with BCI is better than that without BCI. The longitudinal training effect as well as the possible underlying neurophysiological mechanisms explored by fMRI and EEG were our main focus to evaluate the BCI training effect.

Resting-state fMRI is a better tool over task-based fMRI on stroke subjects, since it is not subject to changes in task parameters over time and can avoid excessive

motion artifacts during scan [27, 79]. Recent findings indicate an association between resting state FC and upper-extremity control in persons with stroke [30]. Besides, functional connectivity changes were found in sensorimotor network after motor learning [80, 81]. Xu et al. indicated that inter-hemispheric resting state FC between the bilateral primary sensorimotor cortex was associated with motor recovery in stroke subjects [82]. In order to explore the FC changes within the sensorimotor network, we set two seeds at bilateral primary motor cortex, respectively. Consistent with previous studies, our study also showed a significant modulation of the FC between ipsilesional M1 and contralesional BA6 (premotor cortex and supplementary motor area). This neurological change was futher highly correlated with behavioral changes (FMA score). We have the assumption that the modulation of neuroplasticity is one of the underlying reasons of motor function improvement. FC could serve as a biomarker of motor function recovery in stroke [83], which depicts the functional organization of the brain and neuroplasticity. The significant correlation between motor function improvement and FC change indicated that iM1 and contralesional BA6 could be regarded as the related areas to facilitate upper-limb motor recovery after stroke. Although no significant cluster was survived after correction when the seed was at contralesional M1 after GRF correction, we could still see some positive inter-hemispheric changes in the uncorrected t-map. Some studies indicate that decreased inter-hemispheric connectivity between homologous areas tends to return back to normal in patients who recovered well, whereas in poorly recovered patients, the degree of decreased inter-hemispheric connectivity correlates with motor function [30, 84]. Our results further validate that inter-hemispheric FC changes within sensorimotor network could be an indicator of motor recovery in chronic stroke subjects.

Given the low temporal resolution of fMRI, EEG could be another compensation perspective to capture the neuronal activity and dynamic brain processes more precisely. Plenty of coherence analysis and functional connectivity were conducted from EEG data to explore the potential correlation with motor function or rehabilitation training effect for stroke survivors. Recent findings illustrated that coherence with the primary motor area (M1) of the dominant hemisphere was a strong predictor of motor skill acquisition and thus could provide more information than that predicted by baseline behavior and demographics [85]. Besides, more and more studies focused

on the effective connectivity which can provide directional information compared with coherence-related coupling measurements. It was observed that connectivity from contralesional prefrontal cortex as well as from ipsilesional prefrontal cortex to premotor cortex positively correlated with hand function [29]. In our study, the effective connectivity, named GPDC, was used to explore the relationship between the training effect and information flow within brain functional regions. Similar to previous studies, we found the influence (characterized by information flow defined in GPDC) from cPMA to iM1 significantly correlated with motor recovery. Meanwhile, a strong but not significant correlation between the influence from SMA to iM1 and recovery was also observed.

Considering the findings from previous studies that stroke patients obtained weaker effective connection from cPMA to iM1 during motor imagery and execution compared with healthy subjects [86], our result validated this point from another perspective by showing that the enhanced effective interaction from cPMA to iM1 implied a better rehabilitation recovery. This maybe partially due to the motor imagery procedure of the training therapy since the premotor cortex has been identified as the key node of motor imagery [87]. Our findings additionally suggest that effective connectivity from SMA to iM1 may also be a potential indicator for better recovery. This is not beyond our expectation since together with cPMA, these areas are well known to be involved in planning, initiation and execution of motor commands [88]. It is worth noting that effective connectivity methods (e.g. GPDC) can provide concrete information of the active directed physical links between structures [89]. From this point, repairment or enhancement of these physical connections between motor-related regions should be crucial for recovery, which provides insights into therapy design for stroke rehabilitation. With the popularity of transcranial electrical stimulation recently, our study may provide some insights about the optimization of electrodes montage to facilitate the training effect.

Combined with the result from fMRI, we could find that such concurrent collected EEG could provide more complementary information and disentangle the directionality of the functional connectivity extracted from fMRI. On the other hand, the significant correlation between FC change and directed information flow change within cPMA as well as SMA and iM1 also implied the inherent connection

between these two neuroimaging modalities, which is in line with previous studies [90, 91].

Several limitations need to be noted in our current study. First of all, the sample size was not large limiting the generalization power. More patients should be recruited to validate and extend the findings of this study. Second, EEG data were analyzed at the electrode level. Although surface Laplace filter was used to minimize the volume conduction effect, it might be better to analyze the signal from source perspective and more precise information can be digged out. Finally, our training system comprised motor imagery and robot hand training simultaneously, which lacks a control group. To further differentiate and compare the effect of neuroplasticity modulation and motor recovery brought by different interventions, we could additionally have robot-assist training group and conventional training group in a randomized controlled trial study.

Conclusion

In summary, we investigated the relationship between the motor improvement induced by BCI robot-hand training and functional reorganization from hemodynamic together with electrophysical changes in motor-related regions through concurrent EEG and fMRI. Training effect significantly correlated with functional connectivity change between ipsilesional M1 and contralesional Brodmann area 6 derived from resting-state fMRI. Moreover, significant correlation was observed between motor improvement and information flow changes underlying crucial motor-related area from EEG. Meanwhile, the corresponding changes from EEG and fMRI also illustrated significant revelance which implicated the inherent connection between these two neuroimaging modalities. This study has far-reaching implications for facilitating understanding the potential neural mechanisms during stroke motor recovery.

List of abbreviations

BCI: Brain-computer interface; fMRI: functional magnetic resonance imaging; EEG: electroencephalography; iM1: ipsilesional M1; cPMA: contralesional premotor area; SMA: supplementary motor area; MI: motor imagery; MMSE: Mini–Mental State Examination; FC: functional connectivity; BOLD: blood oxygen level dependent; GPDC: generalized partial directed coherence; FMA: Fugl-Meyer Assessment for upper-extremity; ERD: event-related desynchronization; ECG: electrocardiogram; EOG: electrooculogram; EMG: Electromyography; DPARSF: Data Processing Assistant for Resting-State fMRI; SPM: Statistical Parametric Mapping; CSF: cerebrospinal fluid; MNI: Montreal Neurological Institute; FWMH: full-width at half-maximum; GLM: general linear model; SNR: signal to noise ratio; PCA: principle component analysis; AMICA: adaptive mixture independent component analysis; ROIs: regions of interest; MVAR: multivariate autoregressive; IF: information flow.

Acknowledgements

The authors would like to thank all stroke subjects in this study.

Funding

This study is supported by General Research Fund (Reference No. 14207617), Research Grant Council of Hong Kong.

Ethics approval and consent to participate

This study was approved by the Joint Chinese University of Hong Kong-New Territories East Cluster (CUHK-NTEC) Clinical Research Ethics Committee (registered at https://clinicaltrials.gov (NCT02323061)) and fulfilled the principles of the Declaration of Helsinki. Written informed consent was given before experiments for all subjects.

Availability of data materials

The raw data, including the EEG/fMRI were disclosed for individual subjects. It has been stated in the consent approved by the Joint Chinese University of Hong Kong-New Territories East Cluster (CUHK-NTEC) Clinical Research Ethics Committee that the results might be published, but the individual data would be kept confidentially for subjects.

Author's contributions

KY conducted the experiments, performed signal processing, and prepared the manuscripts. CC conducted the experiments, performed signal processing, and prepared the manuscripts. XW offered signal processing technical support and gave valuable suggestions to polish the manuscripts. WCWC gave valuable suggestions to polish the manuscripts. KYT oversaw and proposed this study, assisted to conduct the experiments, and prepare the manuscripts. All authors read and approved the final manuscript.

Competing interests

The authors declare that they have no competing interests.

Consent for publication

The stroke subjects agreed to the publication of personal demographics and clinical data.

Author details

[1]Department of Biomedical Engineering, The Chinese University of Hong Kong, Shatin, Hong Kong. [2]Department of Imaging and Interventional Radiology, The Chinese University of Hong Kong, Shatin, Hong Kong.

References

1. Langhorne P, Bernhardt J, Kwakkel G. Stroke rehabilitation. The Lancet. 2011;377(9778):1693 – 1702.
2. Wade D. Measurement in neurological rehabilitation. Current opinion in neurology and neurosurgery. 1992 October;5(5):682—686.
3. Norouzi-Gheidari N, Archambault PS, Fung J. Effects of robot-assisted therapy on stroke rehabilitation in upper limbs; Systematic review and meta-analysis of the literature. Journal of Rehabilitation Research and Development. 2012;49(4):479—495.
4. Seitz R, Huang Y, Knorr U, Tellmann L, Herzog H, Freund H. Large-scale plasticity of the human motor cortex. Neuroreport. 1995 March;6(5):742—744.
5. Johansson BB. Current trends in stroke rehabilitation. A review with focus on brain plasticity. Acta Neurologica Scandinavica. 2011;123(3):147–159.
6. Brewer L, Horgan F, Hickey A, Williams D. Stroke rehabilitation: recent advances and future therapies. QJM: An International Journal of Medicine. 2012 09;106(1):11–25.
7. Hummel FC, Cohen LG. Non-invasive brain stimulation: a new strategy to improve neurorehabilitation after stroke? The Lancet Neurology. 2006;5(8):708 – 712.
8. Crozier J, Roig M, Eng J, MacKay-Lyons M, Fung J, Ploughman M, et al. High-Intensity Interval Training After Stroke: An Opportunity to Promote Functional Recovery, Cardiovascular Health, and Neuroplasticity. Neurorehabilitation and Neural Repair. 2018 04;32:154596831876666.

9. Martins J, Aguiar L, Nadeau S, Scianni A, Teixeira-Salmela L, Faria C. Efficacy of task-specific training on physical activity levels of people with stroke: Protocol for a randomized controlled trial. Physical Therapy. 2017 06;97:640–648.
10. Duret C, Grosmaire ag, Krebs H. Robot-Assisted Therapy in Upper Extremity Hemiparesis: Overview of an Evidence-Based Approach. Frontiers in Neurology. 2019 04;10.
11. Rosenthal O, Wing A, Wyatt J, Punt D, Ko-Ko C, Brownless B. Boosting robot-assisted rehabilitation of stroke hemiparesis by individualized selection of upper limb movements - A pilot study. Journal of NeuroEngineering and Rehabilitation. 2019 03;16:42.
12. Silvoni S, Ramos-Murguialday A, Cavinato M, Volpato C, Cisotto G, Turolla A, et al. Brain-Computer Interface in Stroke: A Review of Progress. Clinical EEG and Neuroscience. 2011;42(4):245–252. PMID: 22208122.
13. Broetz D, Braun C, Weber C, Soekadar SR, Caria A, Birbaumer N. Combination of Brain-Computer Interface Training and Goal-Directed Physical Therapy in Chronic Stroke: A Case Report. Neurorehabilitation and Neural Repair. 2010;24(7):674–679. PMID: 20519741.
14. Prasad G, Herman P, Coyle D, McDonough S, Crosbie J. Applying a brain-computer interface to support motor imagery practice in people with stroke for upper limb recovery: a feasibility study. Journal of NeuroEngineering and Rehabilitation. 2010 Dec;7(1):60.
15. Caria A, Weber C, Brötz D, Ramos A, Ticini LF, Gharabaghi A, et al. Chronic stroke recovery after combined BCI training and physiotherapy: A case report. Psychophysiology. 2011;48(4):578–582.
16. Young BM, Nigogosyan Z, Remsik A, Walton LM, Song J, Nair VA, et al. Changes in functional connectivity correlate with behavioral gains in stroke patients after therapy using a brain-computer interface device. Frontiers in Neuroengineering. 2014;7:25.
17. Ibáñez J, Monge-Pereira E, Molina-Rueda F, Serrano JI, del Castillo MD, Cuesta-Gómez A, et al. Low Latency Estimation of Motor Intentions to Assist Reaching Movements along Multiple Sessions in Chronic Stroke Patients: A Feasibility Study. Frontiers in Neuroscience. 2017;11:126.
18. Pfurtscheller G, da Silva FHL. Event-related EEG/MEG synchronization and desynchronization: basic principles. Clinical Neurophysiology. 1999;110(11):1842 – 1857.
19. Remsik A, Young B, Vermilyea R, Kiekhoefer L, Abrams J, Elmore SE, et al. A review of the progression and future implications of brain-computer interface therapies for restoration of distal upper extremity motor function after stroke. Expert Review of Medical Devices. 2016;13(5):445–454. PMID: 27112213.
20. Dobkin BH. Brain–computer interface technology as a tool to augment plasticity and outcomes for neurological rehabilitation. The Journal of Physiology. 2007;579(3):637–642.
21. Bundy DT, Wronkiewicz M, Sharma M, Moran DW, Corbetta M, Leuthardt EC. Using ipsilateral motor signals in the unaffected cerebral hemisphere as a signal platform for brain–computer interfaces in hemiplegic stroke survivors. Journal of Neural Engineering. 2012 may;9(3):036011.
22. Biasiucci A, Leeb R, Iturrate I, Perdikis S, Al-Khodairy A, Corbet T, et al. Brain-actuated functional electrical stimulation elicits lasting arm motor recovery after stroke. Nature Communications. 2018 Dec;9(1):2421.
23. Soekadar SR, Birbaumer N, Slutzky MW, Cohen LG. Brain–machine interfaces in neurorehabilitation of stroke. Neurobiology of Disease. 2015;83:172 – 179.
24. Fox MD, Snyder AZ, Vincent JL, Corbetta M, Van Essen DC, Raichle ME. The human brain is intrinsically organized into dynamic, anticorrelated functional networks. Proceedings of the National Academy of Sciences. 2005;102(27):9673–9678.
25. Greicius MD, Krasnow B, Reiss AL, Menon V. Functional connectivity in the resting brain: A network analysis of the default mode hypothesis. Proceedings of the National Academy of Sciences. 2003;100(1):253–258.
26. Vincent JL, Patel GH, Fox MD, Snyder AZ, Baker JT, Van Essen DC, et al. Intrinsic functional architecture in the anaesthetized monkey brain. Nature. 2007 May;447(7140):83–86.
27. Carter AR, Shulman GL, Corbetta M. Why use a connectivity-based approach to study stroke and recovery of function? NeuroImage. 2012;62(4):2271 – 2280. Connectivity.
28. Wang X, Seguin C, Zalesky A, Wong Ww, Chu WCw, Tong RKy. Synchronization lag in post-stroke: Relation to 1 motor function and structural connectivity. Network Neuroscience. 2019;0(ja):1–48.
29. Westlake KP, Nagarajan SS. Functional Connectivity in Relation to Motor Performance and Recovery After Stroke. Frontiers in Systems Neuroscience. 2011;5.

30. Carter AR, Astafiev SV, Lang CE, Connor LT, Rengachary J, Strube MJ, et al. Resting interhemispheric functional magnetic resonance imaging connectivity predicts performance after stroke. Annals of Neurology. 2010;67(3):365–375.
31. Siegel JS, Ramsey LE, Snyder AZ, Metcalf NV, Chacko RV, Weinberger K, et al. Disruptions of network connectivity predict impairment in multiple behavioral domains after stroke. Proceedings of the National Academy of Sciences. 2016;113(30):E4367–E4376.
32. da Silva FL. EEG and MEG: Relevance to Neuroscience. Neuron. 2013;80(5):1112 – 1128.
33. Koenig T, Prichep L, Lehmann D, Sosa PV, Braeker E, Kleinlogel H, et al. Millisecond by Millisecond, Year by Year: Normative EEG Microstates and Developmental Stages. NeuroImage. 2002;16(1):41 – 48.
34. Friston KJ. Functional and Effective Connectivity: A Review. Brain Connectivity. 2011;1(1):13–36. PMID: 22432952.
35. Fasoula A, Attal Y, Schwartz D. Comparative performance evaluation of data-driven causality measures applied to brain networks. Journal of Neuroscience Methods. 2013;215(2):170 – 189.
36. Woodbury ML, Velozo CA, Richards LG, Duncan PW. Rasch Analysis Staging Methodology to Classify Upper Extremity Movement Impairment After Stroke. Archives of Physical Medicine and Rehabilitation. 2013;94(8):1527 – 1533.
37. Pineda JA. The functional significance of mu rhythms: Translating "seeing" and "hearing" into "doing". Brain Research Reviews. 2005;50(1):57 – 68.
38. Oberman LM, McCleery JP, Hubbard EM, Bernier R, Wiersema JR, Raymaekers R, et al. Developmental changes in mu suppression to observed and executed actions in autism spectrum disorders. Social Cognitive and Affective Neuroscience. 2012 02;8(3):300–304.
39. Kuhlman WN. Functional topography of the human mu rhythm. Electroencephalography and Clinical Neurophysiology. 1978;44(1):83 – 93.
40. Choi CS, Lim H, Kim, Kang, Ku. Brain Computer Interface-Based Action Observation Game Enhances Mu Suppression in Patients with Stroke. Electronics. 2019 12;8:1466.
41. Xu K, Huang YY, Duann JR. The Sensitivity of Single-Trial Mu-Suppression Detection for Motor Imagery Performance as Compared to Motor Execution and Motor Observation Performance. Frontiers in Human Neuroscience. 2019 08;13:302.
42. Ono T, Shindo K, Kawashima K, Ota N, Ito M, Ota T, et al. Brain-computer interface with somatosensory feedback improves functional recovery from severe hemiplegia due to chronic stroke. Frontiers in Neuroengineering. 2014;7:19.
43. Perry A, Bentin S. Mirror activity in the human brain while observing hand movements: A comparison between EEG desynchronization in the mu-range and previous fMRI results. Brain Research. 2009;1282:126 – 132.
44. Yan CG, Wang XD, Zuo XN, Zang YF. DPABI: Data Processing & Analysis for (Resting-State) Brain Imaging. Neuroinformatics. 2016 Jul;14(3):339–351.
45. Friston KJ, Williams S, Howard R, Frackowiak RSJ, Turner R. Movement-Related effects in fMRI time-series. Magnetic Resonance in Medicine. 1996;35(3):346–355.
46. Power JD, Barnes KA, Snyder AZ, Schlaggar BL, Petersen SE. Spurious but systematic correlations in functional connectivity MRI networks arise from subject motion. NeuroImage. 2012;59(3):2142 – 2154.
47. Auer DP. Spontaneous low-frequency blood oxygenation level-dependent fluctuations and functional connectivity analysis of the 'resting' brain. Magnetic Resonance Imaging. 2008;26(7):1055 – 1064. Proceedings of the International School on Magnetic Resonance and Brain Function.
48. Zuo XN, Martino AD, Kelly C, Shehzad ZE, Gee DG, Klein DF, et al. The oscillating brain: Complex and reliable. NeuroImage. 2010;49(2):1432 – 1445.
49. Wu J, Quinlan E, Dodakian L, McKenzie A, Kathuria N, Zhou R, et al. Connectivity Measures Are Robust Biomarkers Of Cortical Function And Plasticity After Stroke. Brain : a journal of neurology. 2015 06;138.
50. Hong X, Lu Z, Teh I, Nasrallah F, Teo WP, Ang K, et al. Brain plasticity following MI-BCI training combined with tDCS in a randomized trial in chronic subcortical stroke subjects: A preliminary study. Scientific Reports. 2017 08;7:9222.
51. Siegel JS, Power JD, Dubis JW, Vogel AC, Church JA, Schlaggar BL, et al. Statistical improvements in functional magnetic resonance imaging analyses produced by censoring high-motion data points. Human Brain

Mapping. 2014;35(5):1981–1996.

52. Wang L, Yu C, Chen H, Qin W, He Y, Fan F, et al. Dynamic functional reorganization of the motor execution network after stroke. Brain. 2010 03;133(4):1224–1238.
53. Vahdat S, Darainy M, Thiel A, Ostry DJ. A Single Session of Robot-Controlled Proprioceptive Training Modulates Functional Connectivity of Sensory Motor Networks and Improves Reaching Accuracy in Chronic Stroke. Neurorehabilitation and Neural Repair. 2019;33(1):70–81. PMID: 30595082.
54. Chen X, Lu B, Yan CG. Reproducibility of R-fMRI metrics on the impact of different strategies for multiple comparison correction and sample sizes. Human Brain Mapping. 2018;39(1):300–318.
55. Delorme A, Makeig S. EEGLAB: an open source toolbox for analysis of single-trial EEG dynamics including independent component analysis. Journal of Neuroscience Methods. 2004;134(1):9 – 21.
56. Oostenveld R, Fries P, Maris E, Schoffelen JM. FieldTrip: Open Source Software for Advanced Analysis of MEG, EEG, and Invasive Electrophysiological Data. Computational intelligence and neuroscience. 2011 01;2011:156869.
57. Niazy RK, Beckmann CF, Iannetti GD, Brady JM, Smith SM. Removal of FMRI environment artifacts from EEG data using optimal basis sets. NeuroImage. 2005;28(3):720 – 737.
58. Liu Z, de Zwart JA, van Gelderen P, Kuo LW, Duyn JH. Statistical feature extraction for artifact removal from concurrent fMRI-EEG recordings. NeuroImage. 2012;59(3):2073 – 2087.
59. Palmer JA, Kreutz-Delgado K, Makeig S. Super-Gaussian Mixture Source Model for ICA. In: Rosca J, Erdogmus D, Príncipe JC, Haykin S, editors. Independent Component Analysis and Blind Signal Separation. Berlin, Heidelberg: Springer Berlin Heidelberg; 2006. p. 854–861.
60. Makeig S, Bell AJ, Jung TP, Sejnowski TJ. Independent Component Analysis of Electroencephalographic Data. In: Touretzky DS, Mozer MC, Hasselmo ME, editors. Advances in Neural Information Processing Systems 8. MIT Press; 1996. p. 145–151.
61. Perrin F, Pernier J, Bertnard O, Giard MH, Echallier JF. Mapping of scalp potentials by surface spline interpolation. Electroencephalography and Clinical Neurophysiology. 1987;66(1):75 – 81.
62. Cohen MX. Analyzing neural time series data: theory and practice. Issues in clinical and cognitive neuropsychology. Cambridge, Massachusetts: The MIT Press; 2014.
63. Gerloff C, Richard J, Hadley J, Schulman AE, Honda M, Hallett M. Functional coupling and regional activation of human cortical motor areas during simple, internally paced and externally paced finger movements. Brain. 1998 Aug;121(8):1513–1531.
64. Granger CWJ. Investigating Causal Relations by Econometric Models and Cross-spectral Methods. Econometrica. 1969;37(3):424–438.
65. Baccala LA, Sameshima K, Takahashi DY. Generalized Partial Directed Coherence. In: 2007 15th International Conference on Digital Signal Processing; 2007. p. 163–166.
66. Kay SM. Modern Spectral Estimation: Theory and Application/Book and Disk. Prentice-Hall Signal Processing Series: Advanced monographs. PTR Prentice Hall; 1988.
67. Thomson DJ. Spectrum estimation and harmonic analysis. Proceedings of the IEEE. 1982 Sep;70(9):1055–1096.
68. Coito A, Genetti M, Pittau F, Iannotti GR, Thomschewski A, Höller Y, et al. Altered directed functional connectivity in temporal lobe epilepsy in the absence of interictal spikes: A high density EEG study. Epilepsia. 2016;57(3):402–411.
69. Astolfi L, Cincotti F, Mattia D, De Vico Fallani F, Tocci A, Colosimo A, et al. Tracking the Time-Varying Cortical Connectivity Patterns by Adaptive Multivariate Estimators. IEEE Transactions on Biomedical Engineering. 2008 March;55(3):902–913.
70. Pagnotta MF, Plomp G. Time-varying MVAR algorithms for directed connectivity analysis: Critical comparison in simulations and benchmark EEG data. PLOS ONE. 2018 06;13(6):1–27.
71. Groppe DM, Bickel S, Keller CJ, Jain SK, Hwang ST, Harden C, et al. Dominant frequencies of resting human brain activity as measured by the electrocorticogram. NeuroImage. 2013;79:223 – 233.
72. Wittmann F, Held J, Lambercy O, Starkey M, Curt A, Höver R, et al. Self-directed arm therapy at home after stroke with a sensor-based virtual reality training system. Journal of NeuroEngineering and Rehabilitation. 2016 08;13:75.

73. Pan H, Yang WW, Kao CL, Tsai M, Wei SH, Fregni F, et al. Effects of 8-week sensory electrical stimulation combined with motor training on EEG-EMG coherence and motor function in individuals with stroke. Scientific Reports. 2018 12;8.
74. Perez-Marcos D, Chevalley O, Schmidlin T, Gangadhar G, Serino A, Vuadens P, et al. Increasing upper limb training intensity in chronic stroke using embodied virtual reality: A pilot study. Journal of NeuroEngineering and Rehabilitation. 2017 12;14.
75. Kim T, Kim S, Lee B. Effects of Action Observational Training Plus Brain–Computer Interface-Based Functional Electrical Stimulation on Paretic Arm Motor Recovery in Patient with Stroke: A Randomized Controlled Trial. Occupational Therapy International. 2016;23(1):39–47. Available from: https://onlinelibrary.wiley.com/doi/abs/10.1002/oti.1403.
76. van Dokkum LEH, Ward T, Laffont I. Brain computer interfaces for neurorehabilitation – its current status as a rehabilitation strategy post-stroke. Annals of Physical and Rehabilitation Medicine. 2015;58(1):3 – 8. Brain Computer Interfaces (BCIs) / Coordinated by Jacques Luauté and Isabelle Laffont.
77. Daly JJ, Wolpaw JR. Brain–computer interfaces in neurological rehabilitation. The Lancet Neurology. 2008;7(11):1032 – 1043.
78. Brace C. Anatomy & Physiology: The Unity of Form and Function. By Kenneth S Saladin. The Quarterly Review of Biology. 2002;77(1):51–51. Available from: https://doi.org/10.1086/343592.
79. Thiel Alexander, Vahdat Shahabeddin. Structural and Resting-State Brain Connectivity of Motor Networks After Stroke. Stroke. 2015;46(1):296–301.
80. Vahdat S, Darainy M, Milner TE, Ostry DJ. Functionally Specific Changes in Resting-State Sensorimotor Networks after Motor Learning. Journal of Neuroscience. 2011;31(47):16907–16915.
81. Askim T, Indredavik B, Vangberg T, Håberg A. Motor Network Changes Associated With Successful Motor Skill Relearning After Acute Ischemic Stroke: A Longitudinal Functional Magnetic Resonance Imaging Study. Neurorehabilitation and Neural Repair. 2009;23(3):295–304. PMID: 18984831.
82. Xu H, Qin W, Chen H, Jiang L, Li K, Yu C. Contribution of the Resting-State Functional Connectivity of the Contralesional Primary Sensorimotor Cortex to Motor Recovery after Subcortical Stroke. PLOS ONE. 2014 01;9(1):1–9.
83. Zhang Y, Liu H, Wang L. Relationship between functional connectivity and motor function assessment in stroke patients with hemiplegia: a resting-state functional MRI study. Neuroradiology. 2016;58:503–511.
84. Urbin MA, Hong X, Lang CE, Carter AR. Resting-State Functional Connectivity and Its Association With Multiple Domains of Upper-Extremity Function in Chronic Stroke. Neurorehabilitation and Neural Repair. 2014;28(8):761–769. PMID: 24553104.
85. Wu J, Srinivasan R, Kaur A, Cramer SC. Resting-state cortical connectivity predicts motor skill acquisition. NeuroImage. 2014;91:84 – 90.
86. Wang L, Zhang JN, Zhang Y, Yan R, Liu H, Qiu MG. Conditional Granger Causality Analysis of Effective Connectivity during Motor Imagery and Motor Execution in Stroke Patients. BioMed Research International. 2016 01;2016:1–9.
87. Xu L, Zhang H, Hui M, Long Z, Jin Z, Liu Y, et al. Motor execution and motor imagery: A comparison of functional connectivity patterns based on graph theory. Neuroscience. 2014;261:184 – 194.
88. Bajaj S, Butler AJ, Drake D, Dhamala M. Brain effective connectivity during motor-imagery and execution following stroke and rehabilitation. NeuroImage: Clinical. 2015;8:572 – 582.
89. Baccalá LA, Sameshima K. Partial directed coherence: a new concept in neural structure determination. Biological Cybernetics. 2001 May;84(6):463–474.
90. Britz J, Ville DVD, Michel CM. BOLD correlates of EEG topography reveal rapid resting-state network dynamics. NeuroImage. 2010;52(4):1162 – 1170.
91. Brookes MJ, Woolrich M, Luckhoo H, Price D, Hale JR, Stephenson MC, et al. Investigating the electrophysiological basis of resting state networks using magnetoencephalography. Proceedings of the National Academy of Sciences. 2011;108(40):16783–16788.

Figures

Tables

Figure 1 Illustration of the experimental settings and characteristics of subjects. (A) Schematic diagram of the whole training system. (B) Comparison of FMA score among pre-training, post-training and six-month follow-up. Significant changes were seen in pre-training versus post-training and pre-training versus six-month follow-up. Error bars are standard errors. *$p < 0.05$. (C) Lesion distribution of stroke subjects. The color bar represents the number of patients with lesions in the corresponding areas. The annotation of X, Y, Z represented the coordinate of the slice in MNI space. (D) The sequence of training paradigm.

Figure 2 Seed selection and FC analysis result. (A) The color-coded area in the ipsilesional side of brain was significantly activated when subjects were doing the task according to task-based fMRI analysis. (B) The yellow sphere with 5 mm radius represents seed location (iM1) selected for seed-based functional connectivity analysis. The coordinate of iM1 was at (38, -22, 56) in MNI space. (C) Functional connectivity between contralesional BA6 and iM1 seed was significantly changed. The color bar represents Z score. The white numbers aside the images represent the coordinate in MNI space.

Figure 3 Significant correlation was found between FMA score change and functional connectivity change. (A) Illustration of the relationship between motor function change and the FC change. (B) Surface rendering of the clusters (contralesional BA6) which had significant FC change with the ipsilesional M1.

Figure 4 The topography plots of information flow when iM1 set as sink/source regions. The first row represents the iM1 as sink region, where (A) and (B) represent the condition of pre and post training respectively. (C) is the change of information flow after training given iM1 as the sink region. The second row represents the iM1 as the source region, where (D) and (E) denoted the pre/post condition. (F) is the change of information flow given iM1 as the source region. All values were z-normalized across the whole brain for better visualization.

Figure 5 The correlation between FMA score change and information flow change from (A) cPMA to iM1, (B) SMA to iM1, (C) iM1 to cPMA and (D) iM1 to SMA. Each surface rendering aside indicated the information flow.

Figure 6 The correlation between functional connectivity change and information flow change from (A) cPMA to iM1, (B) SMA to iM1.

Table 1 Demographics and clinical properties of the participants.

	Age		Stroke onset	Lesion		Stroke	FMA (Max score: 66)		
No.	range	Gender	(years)	side	Lesion location	type	Pre	Post	Six-month
S1	45-49	M	1	R	MFG, SFG, precentral, supramarginal, SMA	ischemic	19	34	28
S2	65-69	M	8	L	insula, putamen, IFG, temporal pole	hemorrhage	22	27	32
S3	65-69	M	1	R	insula, ITG, IOG, putamen	hemorrhage	13	16	27
S4	60-64	M	3	R	insula, putamen, IFG rolandic operculum	ischemic	16	14	18
S5	45-49	M	0.7	R	ITG, MTG, STG, MOG, angular, supramarginal	hemorrhage	17	25	25
S6	60-64	M	11	L	PLIC, putamen, insula,postcentral,SFG	ischemic	22	24	24
S7	55-59	M	6	R	insula, IFG rolandic operculum	ischemic	13	23	20
S8*	40-44	M	5	R	insula, rolandic operculum, IFG, STG, putamen, temporal pole	hemorrhage	15	17	16
S9	50-54	F	3	L	insula, rolandic operculum, putamen	hemorrhage	34	34	37
S10*	40-44	M	3	R	insula, MTG, STG, temporal pole, putamen, rolandic operculum	hemorrhage	17	20	20
S11	55-59	M	5	L	insula, IFG, putamen	hemorrhage	28	33	24
S12	50-54	M	1	L	putamen, caudate nucleus	ischemic	24	22	22
S13	55-59	M	7	R	putamen,temporal pole, IFG, insula, rolandic operculum	ischemic	20	25	21
S14	45-49	M	1	R	insula, putamen	hemorrhage	34	37	35
	mean±std						21±6.7	25±7	25±6

Abbreviations: F = female; FMA = Fugel-Meyer Assessment for upper limb; IFG = Inferior frontal gyrus; IOG = Inferior occipital gyrus; ITG = Inferior temporal gyrus; L = left hemisphere lesion; M = male; MFG = Middle frontal gyrus; MOG = Middle occipital gyrus; MTG = Middle temporal gyrus; PLIC = Posterior limb of the internal capsule; SFG = superior frontal gyrus; SMA = Supplementary motor area; STG = Superior temporal gyrus; R = right hemisphere lesion.

*The EEG of these two subjects were not further analyzed.

Figures

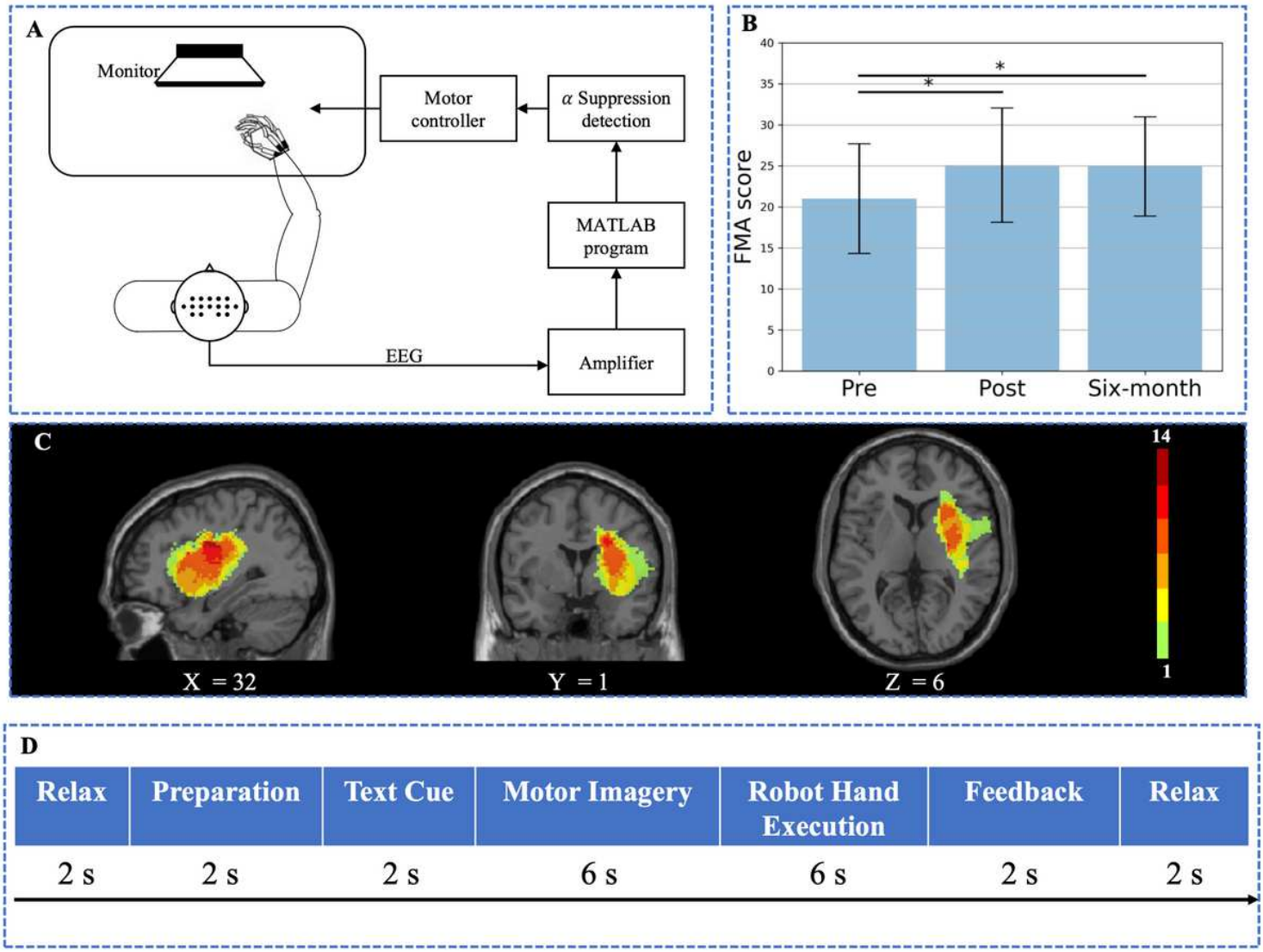

Figure 1

Illustration of the experimental settings and characteristics of subjects. (A) Schematic diagram of the whole training system. (B) Comparison of FMA score among pre-training, post-training and six-month follow-up. Significant changes were seen in pre-training versus post-training and pre-training versus six-month follow-up. Error bars are standard errors. *p < 0.05. (C) Lesion distribution of stroke subjects. The color bar represents the number of patients with lesions in the corresponding areas. The annotation of X, Y, Z represented the coordinate of the slice in MNI space. (D) The sequence of training paradigm.

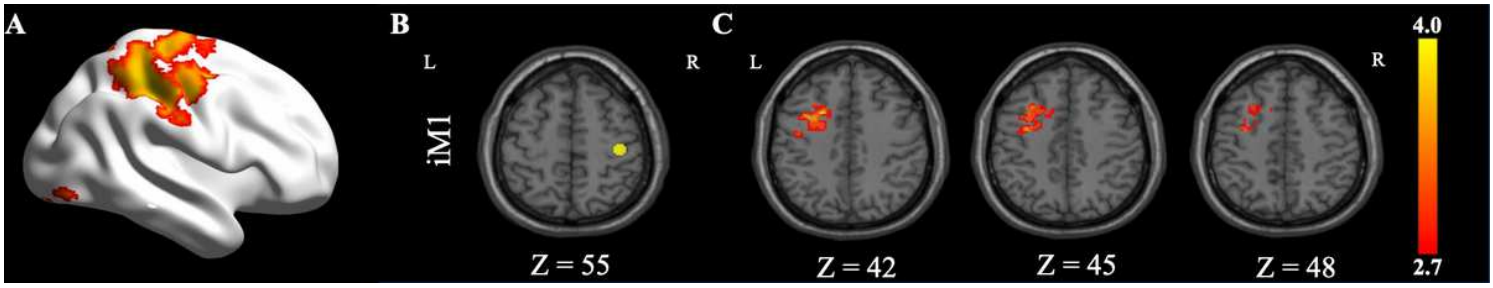

Figure 2

Seed selection and FC analysis result. (A) The color-coded area in the ipsilesional side of brain was significantly activated when subjects were doing the task according to task-based fMRI analysis. (B) The yellow sphere with 5 mm radius represents seed location (iM1) selected for seed-based functional connectivity analysis. The coordinate of iM1 was at (38, -22, 56) in MNI space. (C) Functional connectivity between contralesional BA6 and iM1 seed was significantly changed. The color bar represents Z score. The white numbers aside the images represent the coordinate in MNI space.

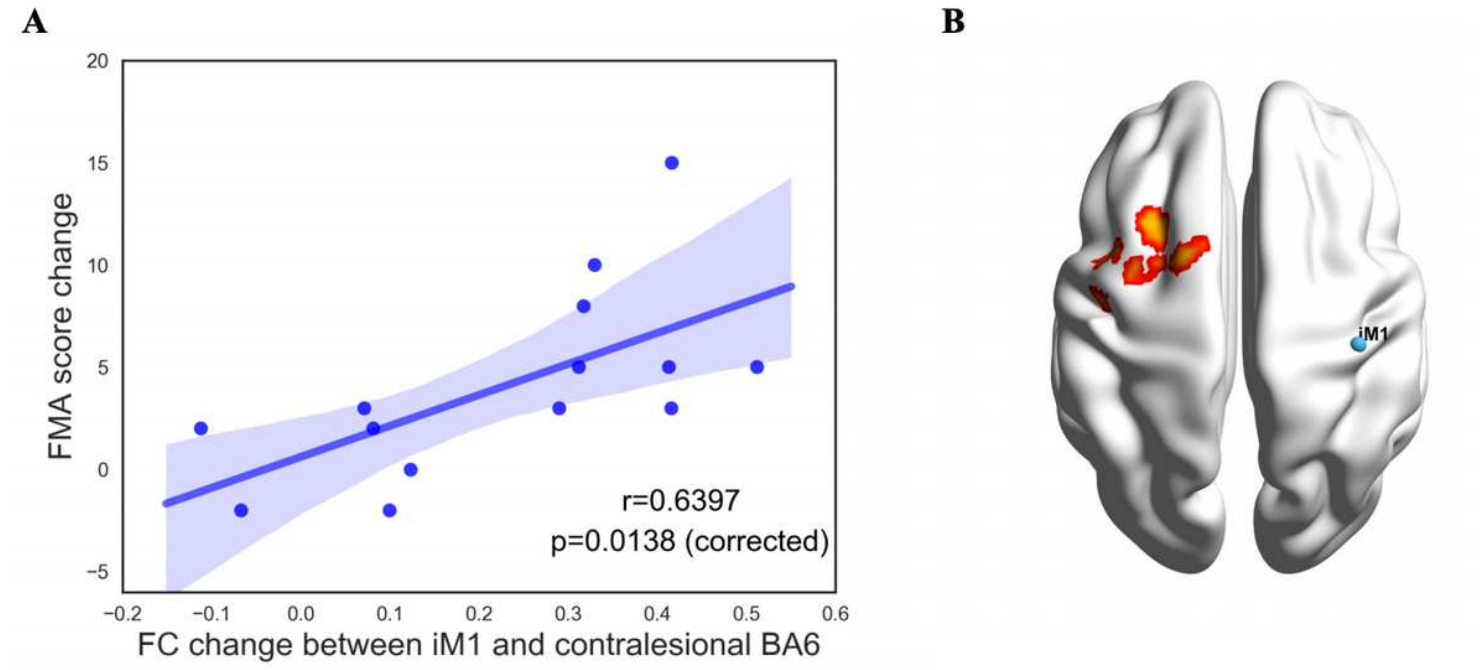

Figure 3

Significant correlation was found between FMA score change and functional connectivity change. (A) Illustration of the relationship between motor function change and the FC change. (B) Surface rendering of the clusters (contralesional BA6) which had significant FC change with the ipsilesional M1.

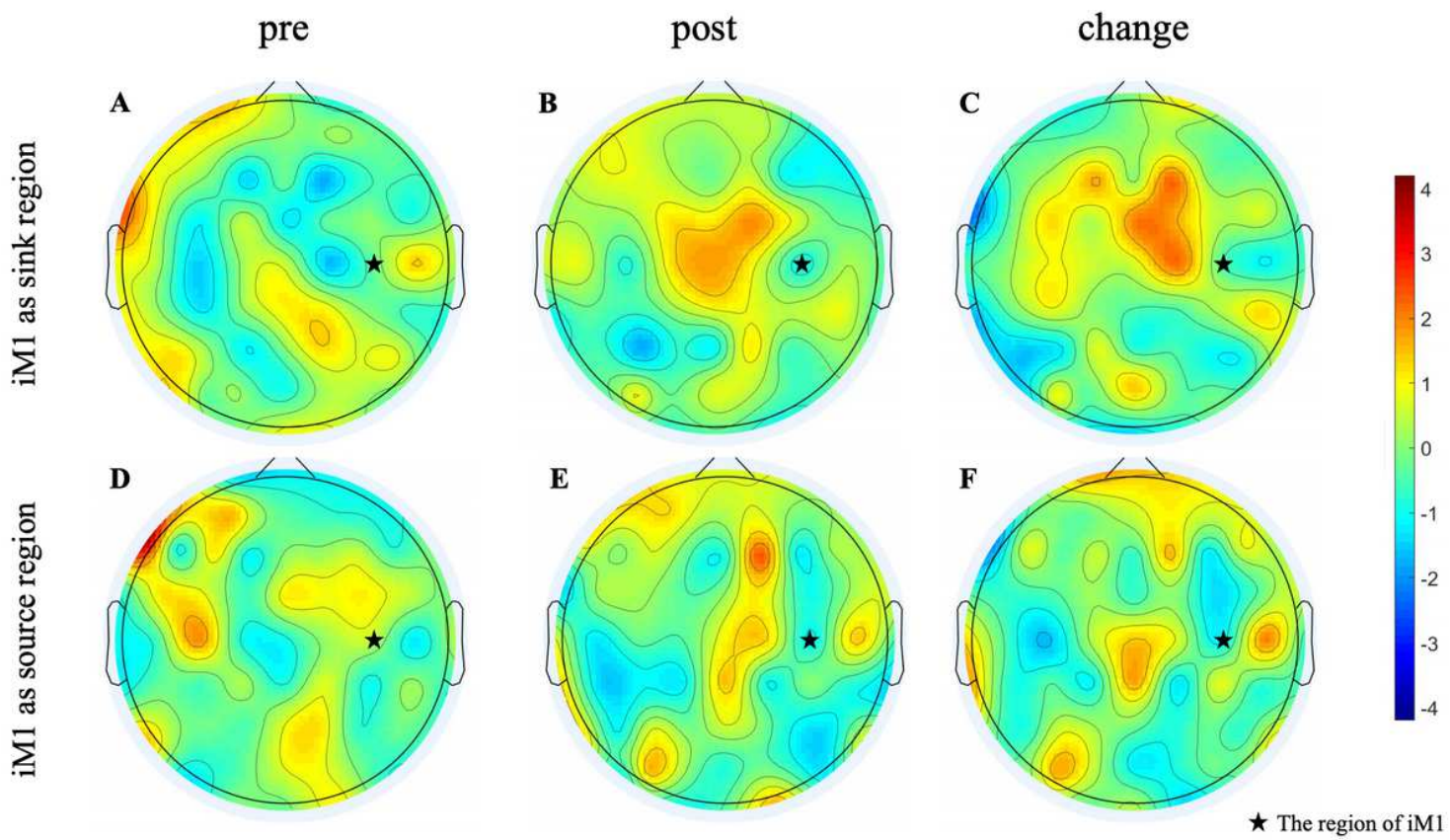

Figure 4

The topography plots of information flow when iM1 set as sink/source regions. The first row represents the iM1 as sink region, where (A) and (B) represent the condition of pre and post training respectively. (C) is the change of information flow after training given iM1 as the sink region. The second row represents the iM1 as the source region, where (D) and (E) denoted the pre/post condition. (F) is the change of information flow given iM1 as the source region. All values were z-normalized across the whole brain for better visualization.

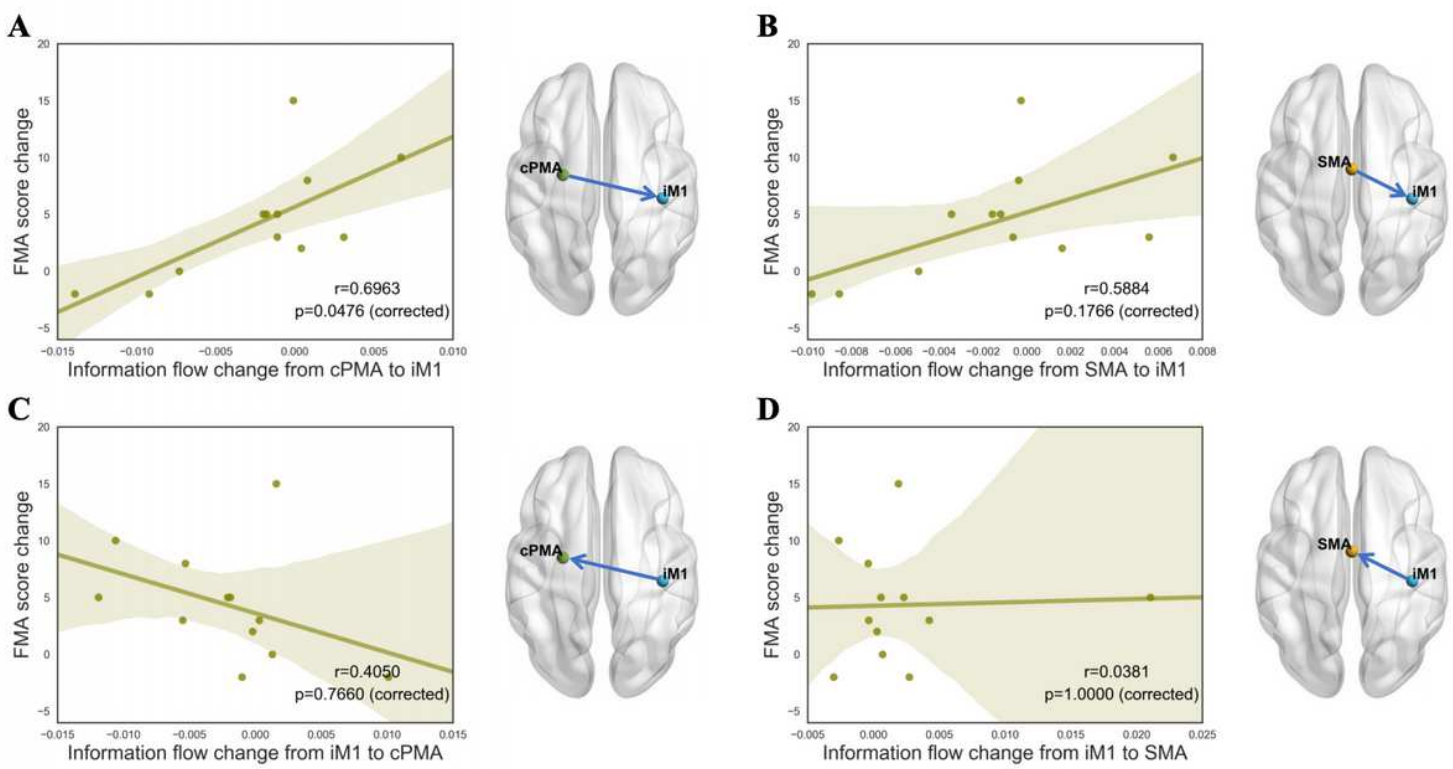

Figure 5

The correlation between FMA score change and information flow change from (A) cPMA to iM1, (B) SMA to iM1, (C) iM1 to cPMA and (D) iM1 to SMA. Each surface rendering aside indicated the information flow.

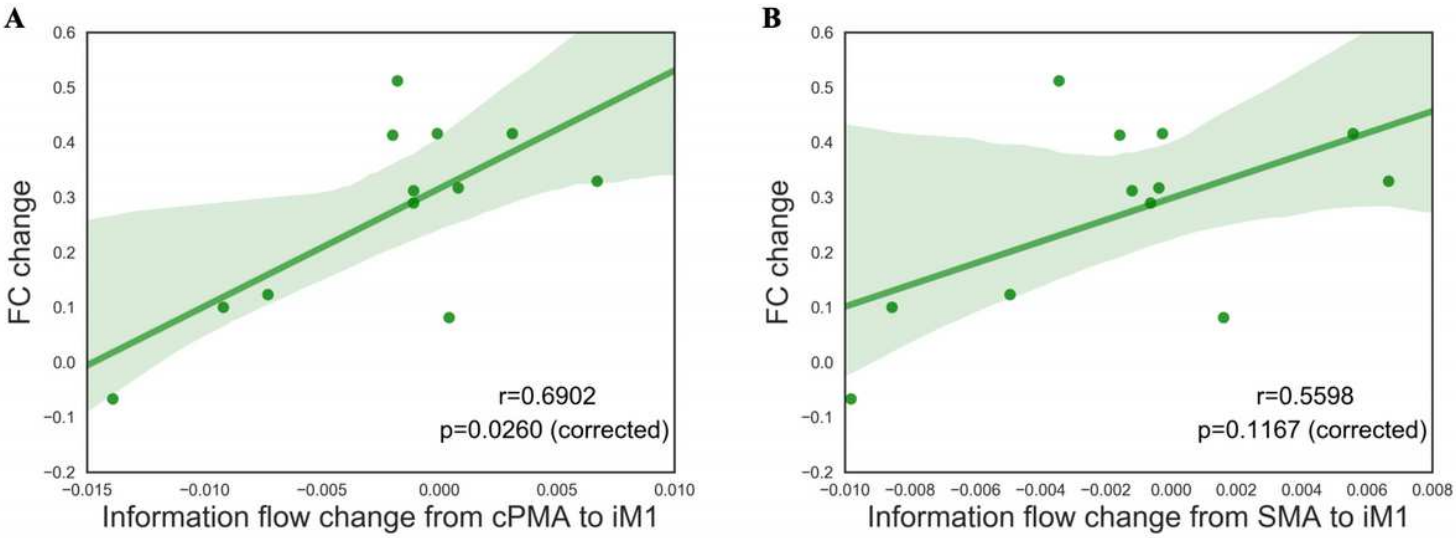

Figure 6

The correlation between functional connectivity change and information flow change from (A) cPMA to iM1, (B) SMA to iM1.